

Improving the morphological stability of a polycrystalline tungsten nanowire with a carbon shell

This article has been downloaded from IOPscience. Please scroll down to see the full text article.

2010 Nanotechnology 21 195701

(<http://iopscience.iop.org/0957-4484/21/19/195701>)

View [the table of contents for this issue](#), or go to the [journal homepage](#) for more

Download details:

IP Address: 137.132.123.69

The article was downloaded on 20/04/2010 at 03:58

Please note that [terms and conditions apply](#).

Improving the morphological stability of a polycrystalline tungsten nanowire with a carbon shell

Guo Feng You¹, Hao Gong² and John T L Thong^{1,3}

¹ Department of Electrical and Computer Engineering, National University of Singapore,

4 Engineering Drive 3, 117576, Singapore

² Department of Materials Science and Engineering, National University of Singapore,

7 Engineering Drive 1, 117574, Singapore

E-mail: elettl@nus.edu.sg (J T L Thong)

Received 25 January 2010, in final form 24 March 2010

Published 19 April 2010

Online at stacks.iop.org/Nano/21/195701

Abstract

Polycrystalline tungsten nanowire is studied for its potential as an interconnect for nanodevices. At elevated temperatures arising from Joule heating at high current densities, a bare 40 nm nanowire was observed *in situ* in a transmission electron microscope to undergo grain grooving that eventually led to its breakage. By overcoating a carbonaceous layer onto the nanowire surface, the tungsten–carbon core–shell structure was found to sustain a much higher current density of about 3×10^7 A cm⁻² before failure, despite significantly higher peak temperature as a result of Joule heating. Failure occurred as a result of a different form of morphological transformation leading finally to breakage by electromigration. These findings suggest that the metal–carbon core–shell structure provides a solution to circumvent morphological instability and increase the current-carrying capability of metallic polycrystalline nanowires.

 Online supplementary data available from stacks.iop.org/Nano/21/195701/mmedia

1. Introduction

Metallic nanowires are very important for nanoscale electronic devices since they serve a vital role as interconnects [1, 2]. As a consequence of diameter scaling down to nanometer levels, interconnects face the challenge of having to bear higher current densities that can lead to electromigration failure as voids or hillocks form [3]. Electromigration is generally considered to arise as a result of momentum transfer between the electron wind and the diffusing metal atoms. This mass transport, in principle, can occur along different diffusion paths, such as lattices, grain boundaries and surfaces which all have distinct activation energies of electromigration [4, 5]. Electromigration is a major reliability issue for nanowire interconnects when the current density approaches values in the range of $\sim 10^6$ – 10^7 A cm⁻² depending on the metallization [6–9].

Moreover, it has been found that the morphology of nanowires becomes unstable and fragments above a certain temperature that is much lower than the melting point of

the material [10–12]. Significant temperature rise as a result of Joule heating at high current densities can lead to morphological instability and present a different mode of interconnect failure. In practice, this effect, which predominates at high temperatures, is not usually observed since metal interconnects are typically in the form of embedded thin films deposited on solid substrates, a configuration which limits the temperature rise as heat dissipates easily from the metallic core.

However, for free-standing nanowire interconnects [13], Joule heating can lead to high temperatures along the length of the nanowire due to the limited thermal conductance of nanowires [14]. For high aspect ratio structures, even relatively low current densities can elevate the temperature sufficiently to cause failure by morphological instability, overtaking electromigration as primary failure mechanism. To date this issue has not received much attention, although it could emerge as a challenge to the use of metal nanowires as interconnects in future nanodevice applications.

In terms of thermal stability, single-crystal nanowires demonstrate high resistance to morphological instability,

³ Author to whom any correspondence should be addressed.

which arises primarily from a Rayleigh instability phenomenon in which the nanowire melts and break into isolated sections [11, 12]. On the other hand, polycrystalline metallic nanowires (PMNWs) are much cheaper candidates for interconnects compared to their single-crystal counterparts, since the synthesis/fabrication of single-crystal metallic nanowires requires very good control of growth conditions which inevitably makes the process costly, thereby limiting their application. While PMNWs are easily realized, they invariably contain, to a lesser or greater extent, grains and grain boundaries which possess large excess free energy. This provides a significant driving force for grain boundary diffusion that can lead to phase transitions and grain growth [15]. Therefore, PMNWs are less thermodynamically stable than their single-crystal counterparts, with a strong tendency to transform into a typical configuration with coarser grain size and fewer interfaces at elevated temperature [16]. For example, a bamboo microstructure is an example of what can result from grain growth in PMNWs [17]. Such bamboo-like PMNWs contain transverse grain boundaries normal to the nanowire axis; the transverse grain boundaries provide an additional source of morphological instability at elevated temperature [18]. The mechanism of this instability is attributed to grain boundary grooving [19, 20], where the depth of the groove progressively increases and the grain boundary neck shrinks until the nanowire finally breaks at the grooving boundary site. When PMNWs are used to carry current that raises the nanowire temperature significantly through Joule heating, a limit on the current carrying capability can be imposed by this form of morphological instability.

In this paper we report a core-shell nanowire structure comprising an amorphous carbonaceous layer coated onto polycrystalline tungsten nanowire. Through *in situ* observations in a transmission electron microscope (TEM) during current stressing, it was found that the current density at which tungsten-carbon (W-C) core-shell nanowires break up is significantly larger than that of bare polycrystalline nanowires. This finding provides a strategy to mitigate the important problem of thermal stability of PMNWs when they are used as current carrying conductors in nanoelectronic devices.

2. Experiment

Polycrystalline tungsten nanowires were grown using the field-emission induced growth (FEIG) method using tungsten hexacarbonyl as the precursor [21]. The growth process was carried out in the chamber of an environmental scanning electron microscope to facilitate immediate viewing during and after nanowire growth. A nanomanipulator was used to contact a positively biased tungsten tip to a grounded electrode on the sample. Under constant-current control, upon breaking the contact between the tip and electrode, an arc discharge initiates the growth of a tip on the electrode from which field emission occurs and nanowire growth proceeds. To grow a nanowire of 40 nm diameter, the field-emission current was set to 500 nA. Samples for *in situ* experiments in the TEM were prepared by growing nanowires on a micromachined silicon die with a through hole. The nanowire straddles the hole and contacts

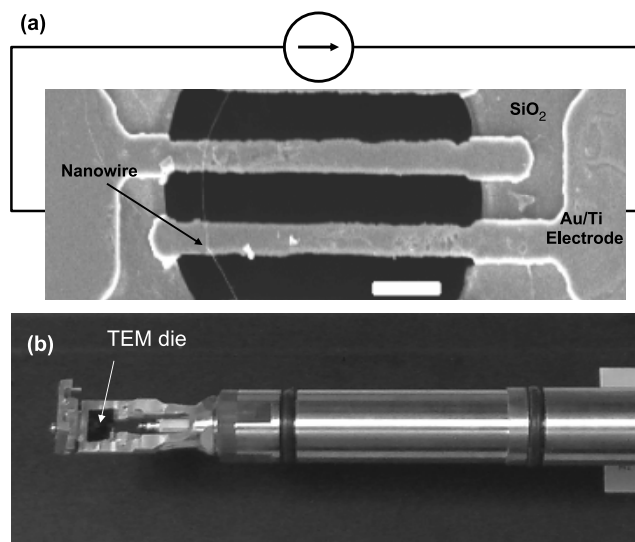


Figure 1. (a) Polycrystalline tungsten nanowire grown on the TEM die (scale bar = 10 μm). (b) Photograph of the TEM sample holder. The TEM die is fitted into the holder with electrical feedthroughs connected to the current source unit.

two Au/Ti electrode bridges that have been patterned on the silicon die with a 100 nm insulating layer of SiO_2 (figure 1(a)). The die fits into a custom-made TEM sample holder (supplied by Nanofactory for a JEOL JEM 2010F TEM) with electrical feedthroughs connected to a current source and control unit (figure 1(b)). This arrangement allows us to supply a current to the nanowire while observing changes to the microstructure.

3. Results and discussion

Figure 2(a) shows a TEM image of an as-grown tungsten nanowire about 40 nm in diameter. The inset indexed diffraction pattern, taken from circled area (indexing PDF no. 04-0806), shows that this nanowire is BCC polycrystalline tungsten containing grains with random crystallographic orientations. In our previous studies, the average grain size was determined by measuring the size of the diffracting nanocrystal in dark-field (DF) images [22]. The average grain size for a nanowire grown at a field-emission current of 500 nA is about 20 nm. Because of the small grain size, the individual nano-sized grains are separated by a high density of grain boundaries ($\sim 10^8 \text{ m}^{-1}$). Therefore the nanowire contains high stored energy [15] that provides the driving force for grain growth at elevated temperatures. A current of 20 μA (corresponding to a current density of about $1.5 \times 10^6 \text{ A cm}^{-2}$) was passed through the wire for 5 min. Due to Joule heating, as the temperature along the nanowire is highest in the middle, TEM images were captured here to observe the most significant morphology changes. Figure 2(b) shows the resulting polycrystalline structure of the nanowire after 5 min of annealing. It can be seen that the grains have grown to straddle the nanowire diameter, resulting in a bamboo-like nanowire structure consisting of individual columnar grains. This structural transformation can be explained by the grain growth model proposed by Frost *et al* [23, 24], which has been

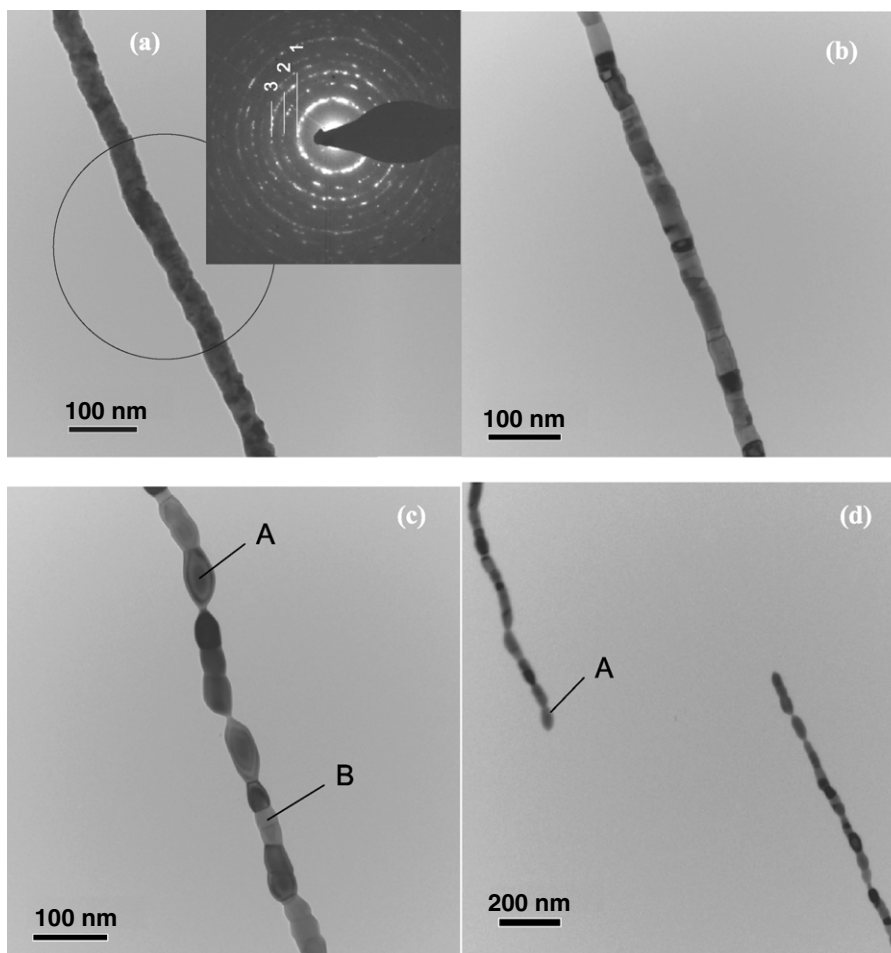


Figure 2. (a) As-grown nanowire; inset shows the SAD pattern. The diffraction rings marked as 1, 2 and 3 correspond to tungsten (110), (200) and (211) planes, respectively. (b) Bamboo-like microstructure formed after current annealing at $20\ \mu\text{A}$ for 5 min. (c) Developed grain grooves after current annealing at $20\ \mu\text{A}$ for 20 min. (d) Nanowire broken at a grain (grain A) with a higher aspect ratio ($L/D \sim 2.86$).

used to simulate the formation of bamboo-like thin-film strips under high temperature annealing [17, 25].

After further annealing (total time of 20 min), grain grooves are seen to have formed between adjacent columnar grains along the line where a grain boundary intersects the surface so that the resultant of the two surface tensions and the grain boundary tension will vanish along the line intersection (figure 2(c)). The formation of the grain groove can be attributed to the tendency of a vertical grain boundary to shrink in order to reduce its area and the free energy [19], so that the grains become pinched-off and spheroidized. After annealing for 25 min, the grooving at some grains (such as grain A) has markedly developed, finally leading to a breakage site (figure 2(d)). Video clips (V1 and V2) provided as supplementary information (available at stacks.iop.org/Nano/21/195701/mmedia) show real-time TEM observations of the development of the grain grooves. This type of break-up feature can be explained by a free energy landscape approach [26]. For a columnar grain with a larger aspect ratio (L/D) of grain length L divided by the grain diameter D , the energy of the grain descends from the initial state to the minimum state of an isolated sphere at elevated temperature (e.g. grain A with $L/D \sim 3$). On the other hand, for a

columnar grain with a small initial aspect ratio (e.g. grain B with $L/D \sim 1.7$) the energy will reach a minimum state wherein the grain still remains connected to its neighbors. In an alternative approach, Klinger and Rabkin simulated the development of grain grooving through calculation from the kinetic process of atomic diffusion on the free surface of a grain [27, 28]. They showed that a critical value $(L/D)_{\text{crit}}$ exists for every grain, above which the grain will break apart from its neighbor. In the present experiment, this critical value $(L/D)_{\text{crit}}$ is about 3 which is in good agreement with this theory ($\sqrt{3/2} < (L/D)_{\text{crit}} < \pi$).

The observed morphological instability of the present polycrystalline tungsten nanowire results from the evolution of grain grooving due to atomic diffusion at the nanowire surface at an elevated temperature as a result of Joule heating. We simulated the temperature along the free-standing tungsten nanowire by solving the thermodynamic function [29]. The maximum simulated temperature is about $850\ ^\circ\text{C}$ at a current density of $1.5 \times 10^6\ \text{A cm}^{-2}$. The thermal conductivity of tungsten nanowire adopted in the simulation is $40\ \text{W m}^{-1}\ \text{K}^{-1}$, which is derived from the Wiedemann–Franz law based on the measured nanowire resistivity of about $50\ \mu\Omega\ \text{cm}$. This simulated temperature corroborates well with independent

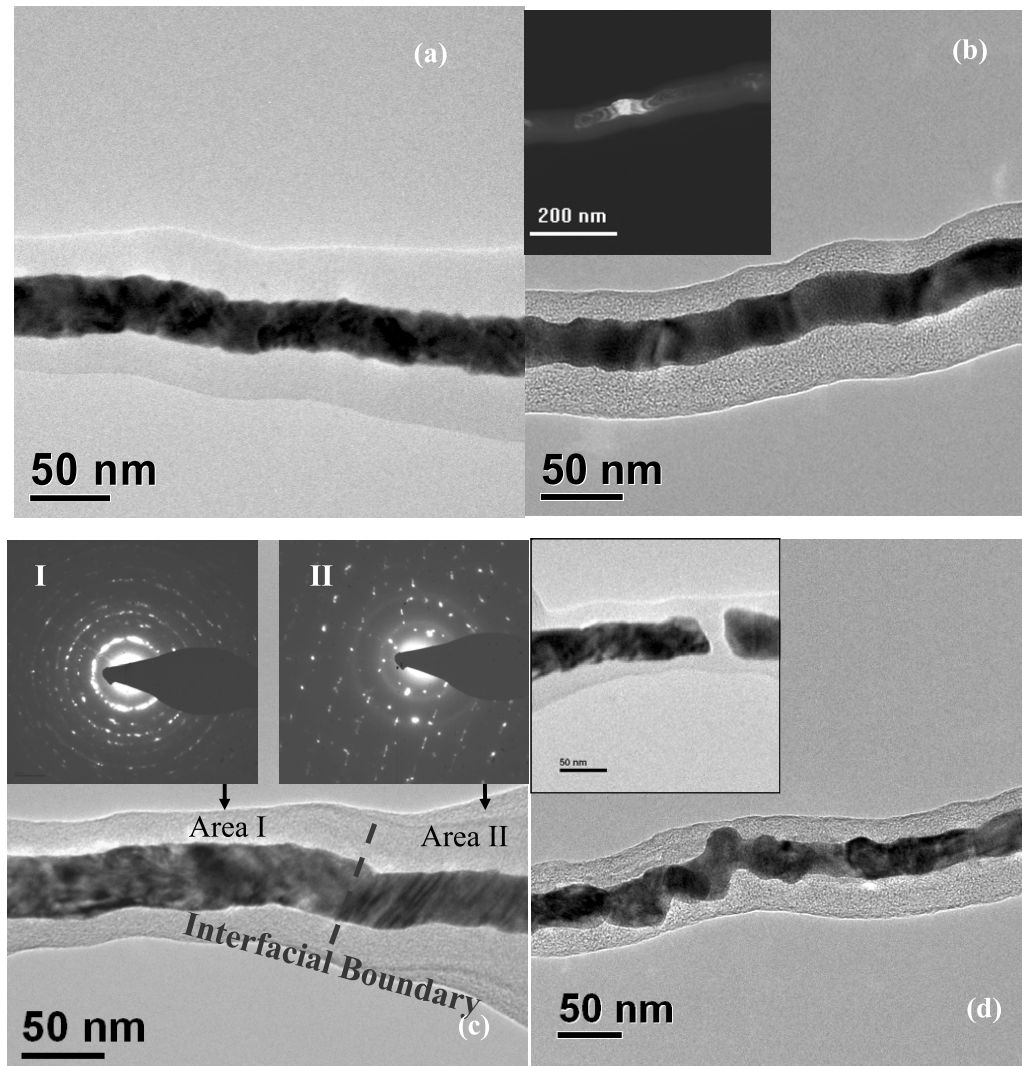


Figure 3. (a) Polycrystalline nanowire coated with a carbonaceous layer. (b) Middle of the nanowire after annealing at $60\ \mu\text{A}$ for 30 min. The inset shows the dark-field image taken using a portion of the W(110) diffraction ring. (c) Interfacial boundary of the nanowire demarcates the polycrystalline portion towards the anchor (Area I) and the single-crystalline portion towards the middle (Area II). (Inset images show the corresponding SAD patterns.) (d) Nanowire after passing a current of $370\ \mu\text{A}$ for 5 min. The inset shows a void formed due to the electromigration in the nanowire.

experiments we carried out on nanowire samples annealed at $850\ ^\circ\text{C}$ on a substrate heater in a high-vacuum system, in which grain grooving of a similar fashion was observed in the TEM. Due to this morphological instability, the maximum current density for time-to-failure of 25 min for the free-standing tungsten PMNW of diameter $40\ \text{nm}$ and length $10\ \mu\text{m}$ is about $1.5 \times 10^6\ \text{A cm}^{-2}$, which is much lower than the current density of about $10^7\ \text{A cm}^{-2}$ for time-to-failure of 20 min for much larger sized submicron thin film tungsten vias and plugs as a result of electromigration failure [6].

Since Joule heating is an unavoidable effect of passing current through a nanowire, one possible way to prevent morphological instability leading to the break-up of the nanowire is to suppress atomic diffusion at the nanowire surface. To this end, a layer of carbonaceous material 20–40 nm thick was coated along the entire length of a tungsten nanowire to form a core-shell structure. The coating was carried out by irradiation in the SEM to deposit contamination

onto the nanowire [30] (figure 3(a)). By scanning the electron beam on one side of the nanowire, the nanowire was homogeneously coated with carbonaceous material (so-called ‘contamination’). It is clearly seen that there are two phases with very different atomic weights and degree of crystallinity. The structure of the cylindrical core is identified from electron diffraction to be mainly BCC tungsten (inset image in figure 2(a)), while the less-dense phase outer shell is believed to be carbonaceous. Through this means, a layer of amorphous carbonaceous material about 20–40 nm thick was coated on the entire length of the tungsten nanowire.

Two-terminal *IV* measurements carried out before and after coating show that the resistivity of the coating is much higher than that of the tungsten core. When the W–C core-shell nanowire structure was stressed with a current of $20\ \mu\text{A}$ (corresponding to an average core current density of $\sim 1.5 \times 10^6\ \text{A cm}^{-2}$) for 30 min, longer than the time of 25 min to break the uncoated tungsten nanowire, no necking is apparent

in the W–C core–shell nanowire. The only notable difference is that the grains have become bigger, as evident from figure 3(b) and the inset dark-field image formed using part of the W(110) diffraction ring. In this instance, the length of the single-crystal grain shown is about 400 nm, which is much larger than the nanowire diameter. To arrive at this state, grain growth must have taken place in the tungsten core through atomic diffusion across the interfacial boundary. The position of the interfacial boundary can be estimated by observing the different selected area diffraction (SAD) patterns emerging on either side of the boundary, as shown in figure 3(c). The SAD pattern in Area II, towards the middle of the nanowire where the temperature is highest, clearly shows single-crystalline nature, as opposed to the polycrystalline nature observed in Area I that is closer to the nanowire anchor. Thus morphological instability due to the grain grooving of the tungsten core has been prevented by the presence of the carbonaceous shell.

It is known that grain grooving at a metal surface is accomplished by material transport through surface diffusion, especially at the beginning of the grain grooving process [19]. Therefore, the prevention of the grain grooving in the W–C core–shell nanowire can be attributed to the inhibition of atomic diffusion at the tungsten–carbon interface. This is different from the case of the free tungsten surface shown in figure 2. According to the bond-order–length–strength (BOLS) correlation theory [31], the critical temperature of the phase transition is proportional to the mean atomic cohesive energy, which is the sum of the bond energy over all the coordination numbers of a given atom, and overheating (defined as increase in the melting temperature T_m) may occur in a substance (the tungsten core here) when it is covered by another substance with higher T_m (the carbonaceous shell). Reaction of the carbon with tungsten at elevated temperature creates interface bonds of carbon and tungsten, and the tungsten core is then overheated. We simulated the temperature along the W–C core–shell nanowire based on experimental measurements of the thermal conductivity of the carbonaceous layer, which is about $3 \text{ W m}^{-1} \text{ K}^{-1}$, less than 10% of $40 \text{ W m}^{-1} \text{ K}^{-1}$ of tungsten nanowire⁴. At a stress current of $20 \mu\text{A}$ (corresponding to an average core current density of $\sim 1.5 \times 10^6 \text{ A cm}^{-2}$), the simulated temperature at the middle of the W–C nanowire is about 800°C , only slightly lower than the peak temperature of the bare tungsten nanowire. Although the temperature of the tungsten nanowire is effectively unchanged after coating with carbonaceous material, since the melting point of the core has been raised by the additional carbonaceous layer, the atomic diffusion at the tungsten–carbon interface will be inhibited at 800°C . Therefore grain grooving does not form in the W–C nanowire unlike the case of the tungsten nanowire at 850°C .

The stress current was increased in increments of $10 \mu\text{A}$. At each current step, thermal grooving in the W–C core–shell nanowire was not observed over a period of 10 min. The only

observed change is a shift in the interfacial boundary towards the nanowire anchor as the single-crystal grain expands. When the stress current increased to about $370 \mu\text{A}$ (equivalent to an average core current density of $\sim 3 \times 10^7 \text{ A cm}^{-2}$), at which the corresponding simulated temperature in middle of the W–C nanowire is about 1400°C , a different form of morphological transformation in the tungsten core started to take place, manifested as roughening of the nanowire as shown in figure 3(d). The inset image shows a gap (void failure) in a W–C nanowire after stressing at a current density of about $3 \times 10^7 \text{ A cm}^{-2}$ for about 5 min. Real-time TEM observation of the development of this gap (video V3 provided as supplementary information available at stacks.iop.org/Nano/21/195701/mmedia) reveals that the void originated at a grain boundary site, where the metal ions are weakly bonded. It can be seen that material is depleted from the grain boundary and transported in the direction of the electron flow (right to left direction in the movie), which is a typical feature of the electromigration phenomenon. Due to the atom flux along the tungsten core, the final broken ends of the tungsten core are almost flat (figure 3(d)). This is in contrast to the morphology of the broken ends of the uncoated bare tungsten nanowire (see figures 2(c) and (d)). In the bare tungsten nanowire, the diameter of the broken ends is much smaller than the average diameter of the wire itself, arising from the progressive shrinkage of the grain boundary grooved neck due to a dominating surface diffusion process.

In summary, the polycrystalline tungsten nanowire of about 40 nm in diameter is morphologically unstable at current of $20 \mu\text{A}$ (equivalent to a current density of about $1.5 \times 10^6 \text{ A cm}^{-2}$) in which the nanowire first transforms to a bamboo microstructure before the development of grain grooving that eventually leads to breakage at the junction of columnar grains with large aspect ratios. This break-up problem is the result of Joule-heating annealing at low current density ($< 1 \times 10^6 \text{ A cm}^{-2}$) passing through the nanowire and can be successfully prevented by overcoating the tungsten core with a carbonaceous layer. With this shell layer, the nanowire can sustain much higher current densities up to $3 \times 10^7 \text{ A cm}^{-2}$. This finding suggests that the W–C core–shell nanowire has great potential for use as a free-standing interconnects in future nanoelectronic devices.

Acknowledgment

This project is support by an NUS research grant R-263-000-419-112.

References

- [1] Xia Y, Yang P, Sun Y, Wu Y, Mayers B, Gates B, Yin Y, Kim F and Yan H 2003 *Adv. Mater.* **15** 353
- [2] Lieber C M and Wang Z L 2007 *MRS Bull.* **32** 99
- [3] Ho P S and Kwok T 1989 *Rep. Prog. Phys.* **52** 301
- [4] Hu C K, Rosenberg R and Lee K Y 1999 *Appl. Phys. Lett.* **74** 2945
- [5] Lloyd J R, Clemens J and Snede R 1999 *Microelectron. Reliab.* **39** 1595
- [6] Tao J, Yong K K, Pico C A and Cheung N W 1991 *IEEE Electron Device Lett.* **12** 646

⁴ To determine the thermal conductivity of the carbonaceous layer, we used a suspended MEMS device [32] to first measure the thermal conductance of a Si nanowire of diameter 300 nm, then repeated the measurement of the thermal conductance after coating the nanowire with a 20 nm thick carbonaceous layer. The difference between the two values is considered as the thermal conductance of the carbonaceous layer.

- [7] Saka M and Ueda R 2005 *J. Mater. Res.* **20** 2712
- [8] Kuan C C, Chien N L, Wen W W and Lih J C 2007 *Appl. Phys. Lett.* **90** 203101
- [9] Huang Q J, Lilley C M and Divan R S 2009 *Nanotechnology* **20** 075706
- [10] Sun Y, Mayers B and Xia Y 2003 *Nano Lett.* **3** 675
- [11] Toimil-Molaes M E, Balogh A G, Cornelius T W, Neumann R and Trautmann C 2004 *Appl. Phys. Lett.* **85** 5337
- [12] Karim S, Toimil-Molaes M E, Balogh A G, Ensinger W, Cornelius T W, Khan E U and Neumann R 2006 *Nanotechnology* **17** 5954
- [13] Oon C H and Thong J T L 2004 *Nanotechnology* **15** 687
- [14] Volz S G and Chen G 1999 *Appl. Phys. Lett.* **75** 2056
- [15] Fecht H J 1990 *Phys. Rev. Lett.* **65** 610
- [16] Klement U, Erb U, El-Sherik A M and Aust K T 1995 *Mater. Sci. Eng. A* **203** 177
- [17] Walton D T, Frost H J and Thompson C V 1992 *Appl. Phys. Lett.* **61** 40
- [18] Klinger L and Rabkin E 2006 *Acta Mater.* **54** 305
- [19] Mullins W W 1957 *J. Appl. Phys.* **28** 33
- [20] Mullins W W 1958 *Acta Metall.* **6** 414
- [21] Thong J T L, Oon C H, Yeadon M and Zhang W D 2002 *Appl. Phys. Lett.* **81** 4823
- [22] Oon C H, Khong S H, Boothroyd C B and Thong J T L 2006 *J. Appl. Phys.* **99** 064309
- [23] Frost H J, Thompson C V, Howe C L and Whang J 1988 *Scr. Metall.* **22** 65
- [24] Frost H J, Thompson C V and Walton D T 1990 *Acta Metall.* **38** 1455
- [25] Hau-Riege C S, Hau-Riege S P and Thompson C V 2001 *J. Electron. Mater.* **30** 11
- [26] Sun B, Suo Z and Cocks C F 1996 *J. Mech. Phys. Solids* **44** 559
- [27] Klinger L and Rabkin E 2005 *Scr. Mater.* **53** 229
- [28] Klinger L and Rabkin E 2005 *Z. Metallkd.* **96** 1119
- [29] Herrero J G, Pascual J I, Mendez J and Baro A M 1993 *Appl. Phys. Lett.* **62** 1077
- [30] Postek M T 1996 *Scanning* **18** 269
- [31] Sun C Q 2007 *Prog. Solid State Chem.* **35** 1
- [32] Shi L, Li D Y, Yu C H, Jang W, Yao Z, Kim P and Majumdar A 2003 *J. Heat Transfer* **125** 881